

## Dynamic nonlinear dielectric response of relaxor ferroelectric $(\text{PbMg}_{1/3}\text{Nb}_{2/3}\text{O}_3)_{0.68}\text{-(PbTiO}_3)_{0.32}$ thin films

M. Tyunina and J. Levoska

*Microelectronics and Materials Physics Laboratories, and EMPART Research Group of Infotech Oulu, University of Oulu, PL 4500, FIN-90014 Oulun yliopisto, Finland*

(Received 1 October 2001; published 26 February 2002)

The dynamic nonlinear dielectric response of relaxor ferroelectric  $(\text{PbMg}_{1/3}\text{Nb}_{2/3}\text{O}_3)_{0.68}\text{-(PbTiO}_3)_{0.32}$  thin films was qualitatively analyzed. The dielectric response of epitaxial thin-film heterostructures deposited on  $\text{La}_{0.5}\text{Sr}_{0.5}\text{CoO}_3/(001)\text{MgO}$  was measured as a function of the amplitude of the ac drive. In thin films, the temperature and frequency dependences of dynamic linear, third-order nonlinear and scaled third-order nonlinear, dielectric permittivities ( $\epsilon_1, \epsilon_3, a_3$ ) were reconstructed from the measured dielectric response of the heterostructures. The behavior of  $\epsilon_1$ ,  $\epsilon_3$ , and  $a_3$  was in qualitative and quantitative agreement with that experimentally observed in single-crystal relaxor ferroelectrics. The peaks in  $\epsilon_1$  and  $\epsilon_3$ , and the increase in  $a_3$  with decreasing temperature below that of the dielectric maximum corresponded to the recent modeling and could indicate a glassy state in the films.

DOI: 10.1103/PhysRevB.65.132101

PACS number(s): 77.84.Dy, 77.55.+f, 77.90.+k, 77.80.Bh

The high potential of relaxor ferroelectrics (RFE) for applications in modern microdevices has stimulated studies of RFE in thin-film form. However, the superb performance of single-crystal RFE has not been reproduced in RFE thin-film heterostructures.<sup>1</sup> In part, this can be ascribed to the influence of interface layers, i.e., thin, low-permittivity dielectric layers near film-electrode interfaces.<sup>2</sup> Besides this factor, in RFE thin films, relatively low processing temperatures and growth strains can result in distortion of the relaxor state itself (e.g., due to a reduced degree of chemical ordering, strain-induced onset of long-range ferroelectric order, etc.). Thus the peculiarities of the relaxor state in thin films become of special interest.

Our recent study<sup>3</sup> of dielectric anomalies in epitaxial films of RFE  $(\text{PbMg}_{1/3}\text{Nb}_{2/3}\text{O}_3)_{0.68}\text{-(PbTiO}_3)_{0.32}$  (PMNT) has revealed that typical features of bulk RFE can be preserved in thin films. In PMNT films, deviation from Curie-Weiss behavior, the Vögel-Fulcher relationship, temperature evolution of the glasslike local order parameter, and temperature evolution of the relaxation time spectrum have been found to be essentially similar to those in single-crystal PMNT. However, according to the latest modeling of RFE,<sup>4-6</sup> the key characteristics of the relaxor state can be obtained by analyzing the dynamic nonlinear dielectric response of RFE.

In particular, the dynamic spherical random-bond-random-field (SRBRF) model<sup>6</sup> predicts frequency-dependent peaks in the third-order dynamic nonlinear susceptibility  $\chi_3(T)$  and in the scaled third-order nonlinear susceptibility  $\chi_3'(f)/\chi_1'(3f)\chi_1'(f)^3$ , where  $\chi_1$  is the dynamic linear susceptibility,  $T$  is the temperature, and  $f$  is the frequency of the sinusoidal oscillating electric field  $E$ . Here  $\chi_1$  and  $\chi_3$  are defined in terms of the expansion of polarization  $P$ :  $P = (\chi_1 E + \chi_3 E^3 + \dots)$ .  $\chi_1'$  and  $\chi_3'$  are the real parts of  $\chi_1$  and  $\chi_3$ , respectively. Earlier, in the phenomenological model,<sup>5</sup> a coefficient  $\beta$  analogous to the scaled third-order nonlinear susceptibility was introduced. A freezing transition into a glasslike state can be indicated by a peak in the scaled third-order nonlinear susceptibility and/or in  $\beta$  around the freezing

temperature  $T_f$ .<sup>5,6</sup> A steep increase in  $\beta$  with decreasing temperature below that of the dielectric maximum has been experimentally observed in single-crystal  $\text{PbMg}_{1/3}\text{Nb}_{2/3}\text{O}_3$ .<sup>5</sup> Peaks in  $\chi_3'$  around  $T_f$  and the frequency dispersion of  $\chi_3'$  at low temperatures have been found in bulk RFE,<sup>5,7,8</sup> in agreement with modeling. The experimental observations<sup>5,7,8,9</sup> suggest the glassy state in bulk RFE.

The purpose of this paper is to identify the RFE state in PMNT thin films by analyzing the dynamic nonlinear response of the films. To study experimentally the dynamic nonlinear response of ceramic or single-crystal bulk RFE, the real and imaginary parts of the first and third harmonics of the dielectric permittivity and/or of polarization are usually measured as a function of  $T$  and  $f$  using an ac field with amplitude  $E_0$  that should be small enough to probe the true RFE state.<sup>5,8,9</sup> In thin films, due to the interface contribution, neither polarization, dielectric permittivity, nor actual electric field can be determined directly from those measured in the heterostructure.<sup>2,3,10</sup> Thus the methods used for studies of the dielectric nonlinearities in bulk RFE cannot be applied to thin films.

As shown recently,<sup>3,10</sup> the real part of the dielectric permittivity of the film,  $\epsilon_f$ , and actual electric field across the film,  $E_f$ , can be reconstructed from the corresponding  $\epsilon_h$  and  $E_h$  in the heterostructure using a trivial model of a series connection of film and interface layer:

$$\frac{1}{\epsilon_f} \cong \frac{1}{\epsilon_h} - \frac{1}{\epsilon_{in}}, \quad (1)$$

$$E_f \cong E_h \left( 1 - \frac{\epsilon_h}{\epsilon_{in}} \right). \quad (2)$$

Here  $\epsilon_{in}$  characterizes the interface contribution:  $\epsilon_{in} = (\epsilon_i/d_i)d_f$ , where  $\epsilon_i$  and  $d_i$  are the dielectric permittivity and thickness of the interface layer, and  $d_f$  is the thickness of the film ( $d_f \gg d_i$ ). Here  $\epsilon_{in}$  can be evaluated as  $\epsilon_{in}$

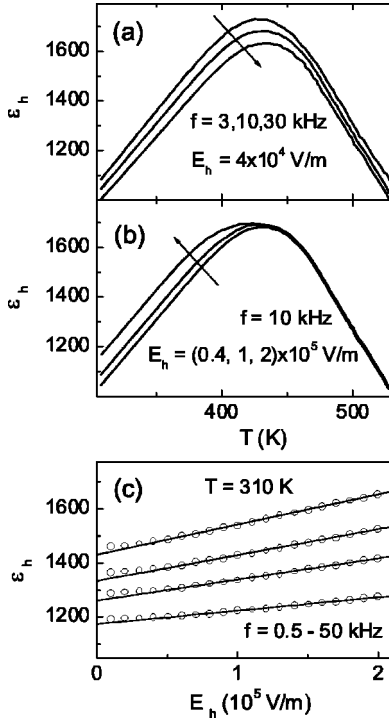


FIG. 1. Dielectric response of Pt/PMNT/La<sub>0.5</sub>Sr<sub>0.5</sub>CoO<sub>3</sub>/MgO heterostructure. The real part of the dielectric permittivity of the heterostructure,  $\varepsilon_h$ : (a, b) as a function of temperature  $T$  measured (a) at frequencies  $f=3, 10,$  and  $30$  kHz from the upper curve down and using the amplitude of the applied ac field,  $E_h=4 \times 10^4$  V/m, and measured (b) at  $f=10$  kHz and  $E_h=0.4, 1,$  and  $2 \times 10^5$  V/m from the lower curve up; (c) as a function of amplitude of applied ac field,  $E_h$ , measured at  $T=310$  K and  $f=0.5, 2, 10,$  and  $50$  kHz from the upper curve down (straight solid lines show the linear fit  $\varepsilon_h \propto E_h$ ). Arrows show direction of increasing  $f$  or  $E_h$ .

$\cong \varepsilon_{mh}/\alpha$ , where  $\varepsilon_{mh}$  is the maximum in  $\varepsilon_h(T)$  and  $\alpha$  is a fitting parameter,  $0.70 < \alpha < 0.99$ .<sup>3</sup>

The nonlinear dielectric response of RFE thin films can be studied by measuring  $\varepsilon_h$  as a function of the amplitude of the applied ac field at different  $f$  and  $T$ . The field dependence of  $\varepsilon_f$  can be reconstructed using Eqs. (1) and (2). Following the phenomenological approach, the RFE behavior of the film should be indicated by a square dependence of  $\varepsilon_f$  on the amplitude of the ac field seen by the film,  $E_f$ , i.e.,

$$\varepsilon_f \cong \varepsilon_1 + \frac{3}{4} \varepsilon_3 E_f^2, \quad (3)$$

where  $\varepsilon_1$  and  $\varepsilon_3$  refer to the dynamic linear permittivity and to the third-order dynamic nonlinear permittivity, respectively, and both  $\varepsilon_1$  and  $\varepsilon_3$  depend on frequency and temperature. By the analogy to the scaled third-order nonlinear susceptibility of the SRBRF model, the coefficient  $a_3$  or scaled dynamic third-order nonlinear dielectric permittivity can be defined as

$$a_3 = \frac{\varepsilon_3(f)}{[\varepsilon_1(f)]^3 \varepsilon_1(3f)}, \quad (4)$$

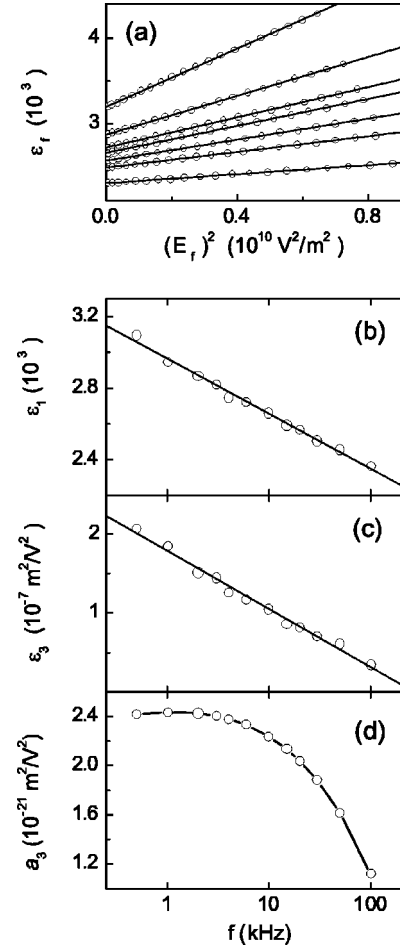


FIG. 2. Reconstructed dielectric response of the PMNT thin film. (a) The real part of the dielectric permittivity of the film,  $\varepsilon_f$ , as a function of the square of the amplitude,  $(E_f)^2$ , of the ac field seen by the film determined at  $T=310$  K and  $f=0.5, 1, 3, 10, 30,$  and  $100$  kHz from the upper curve down. Solid lines show the linear fits  $\varepsilon_f \propto (E_f)^2$ . (b)–(d) The frequency dependence of (b) dynamic linear dielectric permittivity  $\varepsilon_1$ , (c) dynamic third-order nonlinear dielectric permittivity  $\varepsilon_3$ , and (d) scaled third-order nonlinear dielectric permittivity  $a_3$  extracted from the linear fits  $\varepsilon_f \propto (E_f)^2$  in (a).

where  $\varepsilon_1(f)$ ,  $\varepsilon_1(3f)$ , and  $\varepsilon_3(f)$  can be found from the linear fits of  $\varepsilon_f(E_f^2)$  determined at different frequencies and temperatures.

The proposed procedure was used for a qualitative analysis of the dynamic nonlinear dielectric response of PMNT films. Epitaxial heterostructures of (001)-oriented thin (250 nm) films of PMNT with bottom La<sub>0.5</sub>Sr<sub>0.5</sub>CoO<sub>3</sub> and top Pt electrodes were deposited by *in situ* pulsed laser ablation on MgO (001) single-crystal substrates. Details of the deposition and the epitaxial quality of the films can be found elsewhere.<sup>11</sup> Dielectric properties of the heterostructures were studied as a function of amplitude of applied ac field,  $E_h=10^4$ – $10^6$  V/m, in a range of  $f=10^2$ – $10^6$  Hz and  $T=295$ – $600$  K, using an HP4284 A LCR meter.

A typical behavior of  $\varepsilon_h$  directly measured in the heterostructures is represented in Fig. 1. The small-signal  $\varepsilon_h(f, T)$  exhibited [Fig. 1(a)] a broad peak around  $T_m=425$  K and a

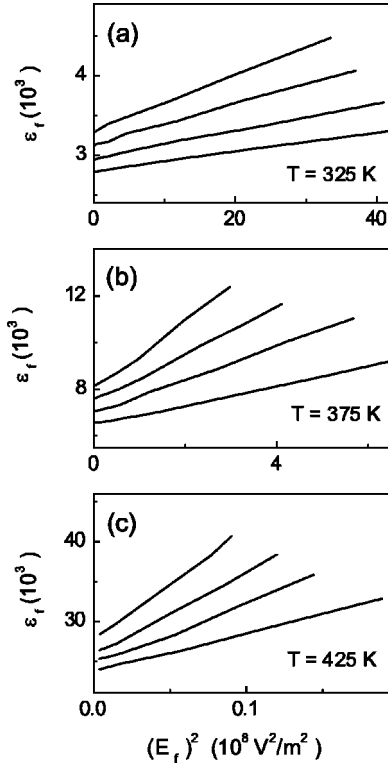


FIG. 3. Reconstructed dielectric response of the PMNT thin film. The real part of the dielectric permittivity of the film,  $\epsilon_f$ , as a function of square of amplitude,  $(E_f)^2$ , of ac field seen by the film determined at  $f=1, 3, 10$ , and  $30$  kHz from upper curves down, at temperatures (a)  $325$  K, (b)  $375$  K, and (c)  $425$  K.

relaxorlike frequency dispersion of  $T_m$  and  $\epsilon_{mh}$ . (More details can be found in Ref. 3.) Increasing the amplitude of the ac drive did not result in a noticeable increase in  $\epsilon_{mh}$  [Fig. 1(b)], in contrast to the observations in bulk PMNT (Ref. 12) and in agreement with our recent estimations.<sup>10</sup> Such a behavior of  $\epsilon_{mh}$  can be understood from Eq. (2): around  $T_m$ , the actual  $E_f$  has a minimum, and an increase in  $E_h$  is accompanied by an increase in  $\epsilon_h$  and, consequently, only a minor change in  $E_f$ . Respectively, weak changes in  $\epsilon_f$  and  $\epsilon_{hm}$  are expected. The RFE-type shift of  $T_m$  to lower temperatures with increasing  $E_h$  was, however, preserved. The dependence of  $\epsilon_h$  on  $E_h$  measured at a fixed temperature below  $T_m$  [Fig. 1(c)] was neither a square nor linear one, also in agreement with Ref. 10.

The actual dependence of  $\epsilon_f$  on  $E_f$  in the film was reconstructed [Fig. 2(a)] using the interface contribution  $\epsilon_{in}$  evaluated from the data in Fig. 1(a). A good linear fit of the obtained dependence of  $\epsilon_f$  on  $(E_f)^2$  was found that revealed the validity of Eq. (3) for the films. From the linear fits of  $\epsilon_f(E_f^2)$  determined at different frequencies, the frequency dependent coefficients  $\epsilon_1(f)$  and  $\epsilon_3(f)$  were extracted [Figs. 2(a) and 2(b)]. The value of  $\epsilon_1(3f)$  was found from the dependence of  $\epsilon_1(f)$ , and the scaled nonlinearity  $a_3$  was calculated [Fig. 2(d)].

To study the temperature evolution of  $\epsilon_1$ ,  $\epsilon_3$ , and  $a_3$ ,  $\epsilon_h$  was measured as a function of  $E_h$  at different  $f$  and different fixed  $T$ . It should be noted that neither thermal hysteresis nor

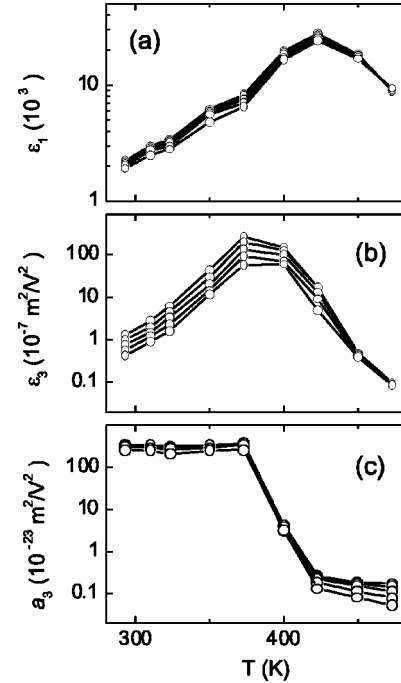


FIG. 4. Temperature evolution of the dynamic nonlinear dielectric response of the PMNT film. (a) Linear dielectric permittivity  $\epsilon_1$ , (b) third-order nonlinear dielectric permittivity  $\epsilon_3$ , and (c) scaled third-order nonlinear dielectric permittivity  $a_3$  as a function of temperature determined at  $f=0.5, 1, 3, 10$ , and  $30$  kHz (from the upper curves down).

hysteresis with respect to  $E_h$  was detected for  $\epsilon_h$ . The corresponding reconstructed dependence of  $\epsilon_f$  on  $(E_f)^2$  remained linear in a broad temperature range (Fig. 3), which made it possible to evaluate  $\epsilon_1$ ,  $\epsilon_3$ , and  $a_3$  using Eqs. (3) and (4). The results are presented in Fig. 4.

Both  $\epsilon_1(T)$  and  $\epsilon_3(T)$  exhibited a maximum below  $T_m$ . An increase in  $\epsilon_3$  by almost three orders of magnitude with decreasing  $T$  below  $T_m$  [Fig. 4(b)] was in agreement with the behavior of  $\chi'_3$  experimentally observed in single-crystal  $\text{PbMg}_{1/3}\text{Nb}_{2/3}\text{O}_3$  using another measurement technique.<sup>5,7</sup> Also a strong frequency dispersion of  $\epsilon_3$  was in agreement with that in  $\chi'_3$ . The magnitude of  $\epsilon_3$  was in agreement with that in bulk RFE.<sup>8</sup>

Generally, the behavior of  $\epsilon_1(T)$  and  $\epsilon_3(T)$  was in a qualitative agreement with the SRBRF model.<sup>6</sup> However, although the exact positions of the maxima in  $\epsilon_1(T)$  and  $\epsilon_3(T)$  could not be detected in the present set of measurements, a somewhat higher temperature of the maximum in  $\epsilon_1$  with respect to that in  $\epsilon_3$  was in contrast to model expectations.<sup>6</sup> In PMNT films, the previously found<sup>3</sup> proximity of  $T_f$  to  $T_m$  and relatively small Curie constant could result from the compressive in-plane stress. It is not clear, however, if the shift of the peak in  $\epsilon_1(T)$  to higher  $T$  (by analogy with the shift of Curie point) might be attributed to this stress.

An increase in  $a_3$  with decreasing  $T$  below  $T_m$  [Fig. 4(c)] was in qualitative agreement with the phenomenological modeling and experimental observations<sup>5</sup> in single-crystal  $\text{PbMg}_{1/3}\text{Nb}_{2/3}\text{O}_3$ . Also, the magnitude of  $a_3$  corresponded to

the magnitude of  $\beta$  in Ref. 5. The observed  $a_3(f, T)$  followed the SRBRF model<sup>6</sup> in part of the obtained increase and frequency dispersion. Neither the expected consequent decrease of  $a_3$  with further decreasing  $T$  nor the low-temperature increase of  $a_3$  could be found. (Assuming the position of maximum in  $\varepsilon_3$  about 390 K, a lower  $a_3$  could be expected at temperatures from 350 to 240 K). Since in the SRBRF model<sup>6</sup> the shape of  $a_3(f, T)$  strongly depends on the probability distribution of relaxation times, such a discrepancy can be attributed to the difference between the assumed distribution and the real one in PMNT films.

In summary, the RFE state of epitaxial PMNT thin films was probed by studying the dynamic nonlinear dielectric

response of the films. In thin films, temperature and frequency dependences of dynamic linear, third-order nonlinear and scaled third-order nonlinear dielectric permittivities  $\varepsilon_1$ ,  $\varepsilon_3$ , and  $a_3$ , respectively, were reconstructed from the dielectric response of the thin-film heterostructures measured as a function of the amplitude of the ac drive. The behavior of  $\varepsilon_1$ ,  $\varepsilon_3$ , and  $a_3$  was in qualitative and quantitative agreement with that experimentally observed in single-crystal RFE. The peaks in  $\varepsilon_1(T)$  and  $\varepsilon_3(T)$  and the increase in  $a_3(T)$  with decreasing  $T$  below  $T_m$  corresponded to the recent modeling and could indicate the glassy state in PMNT films.

The work was supported in part by the Academy of Finland (Project No. 173770).

<sup>1</sup>For the most recent studies see, e.g., Z. Kighelman *et al.*, Appl. Phys. Lett. **73**, 2281 (1998); G.R. Bai *et al.*, *ibid.* **76**, 3106 (2000); V. Nagarajan *et al.*, *ibid.* **77**, 438 (2000); J.P. Maria, W. Hackenberger, and S. Trolier-McKinstry, J. Appl. Phys. **84**, 5147 (1998); V. Bornand and S. Trolier-McKinstry, *ibid.* **87**, 3958 (2000).

<sup>2</sup>S.L. Miller *et al.*, J. Appl. Phys. **68**, 6463 (1990); A.K. Tagantsev *et al.*, *ibid.* **78**, 2623 (1995); C. Zhou and D.M. Newns, *ibid.* **82**, 3081 (1997); O.G. Vendik and S. Zubko, *ibid.* **82**, 4475 (1997); C. Basceri *et al.*, *ibid.* **82**, 2497 (1997); H.C. Li *et al.*, Appl. Phys. Lett. **73**, 464 (1998); A.K. Tagantsev and I.A. Stolichnov, *ibid.* **74**, 1326 (1999); B.T. Lee and C.S. Hwang, *ibid.* **77**, 124 (2000).

<sup>3</sup>M. Tyunina and J. Levoska, Phys. Rev. B **63**, 224102 (2001).

<sup>4</sup>B.E. Vugmeister and H. Rabitz, Phys. Rev. B **61**, 14 448 (2000).

<sup>5</sup>A.E. Glazounov and A.K. Tagantsev, Phys. Rev. Lett. **85**, 2192 (2000).

<sup>6</sup>R. Pirc, R. Blinc, and V. Bobnar, Phys. Rev. B **63**, 054203 (2001).

<sup>7</sup>A. Levstik, Z. Kutnjak, C. Filipič, and R. Pirc, Phys. Rev. B **57**, 11 204 (1998).

<sup>8</sup>V. Bobnar, Z. Kutnjak, and A. Levstik, Appl. Phys. Lett. **76**, 2773 (2000).

<sup>9</sup>V. Bobnar, Z. Kutnjak, R. Pirc, P. Blinc, and A. Levstik, Phys. Rev. Lett. **84**, 5892 (2000).

<sup>10</sup>M. Tyunina, J. Levoska, S. Leppävuori, and A. Sternberg, Appl. Phys. Lett. **78**, 527 (2001).

<sup>11</sup>M. Tyunina, J. Levoska, A. Sternberg, and S. Leppävuori, J. Appl. Phys. **86**, 5179 (1999); J. Levoska, M. Tyunina, A. Sternberg, and S. Leppävuori, Appl. Phys. A **70**, 269 (2000).

<sup>12</sup>E. Colla, S. Gupta, and D. Viehland, J. Appl. Phys. **85**, 362 (1999); E.V. Colla, E.L. Furman, S.M. Gupta, N.K. Yushin, and D. Viehland, *ibid.* **85**, 1693 (1999).